Scientific Papers of
the Department of Electrical Power Engineering of
the Wrocław University of Technology

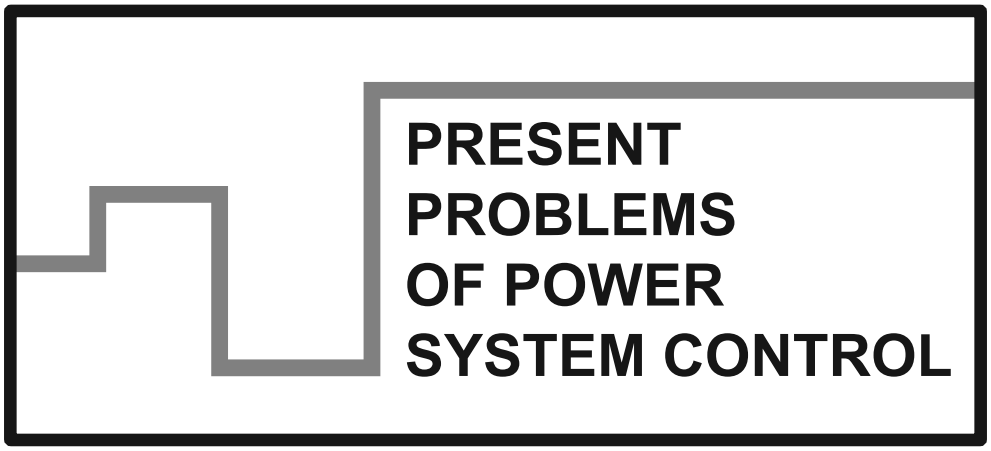

6

Wrocław 2015

Printed in the camera ready form

Department of Electrical Power Engineering
Wrocław University of Technology
Wybrzeże Wyspiańskiego 27, 50-370 Wrocław, Poland
phone: +48 71 320 35 41
www: http://www.weny.pwr.edu.pl/instytuty,52.dhtml; http://www.psc.pwr.edu.pl
e-mail: wydz.elektryczny@pwr.edu.pl

OFICYNA WYDAWNICZA POLITECHNIKI WROCŁAWSKIEJ
Wybrzeże Wyspiańskiego 27, 50-370 Wrocław
http://www.oficyna.pwr.edu.pl
e-mail: oficwyd@pwr.edu.pl
zamawianie.ksiazek@pwr.edu.pl

ISSN 2084-2201

Print and binding: beta-druk, www.betadruk.pl

capacitive voltage transformer,
ferroresonance, suppression circuit,
chaotic behaviour, simulation

Jan IŻYKOWSKI*
Eugeniusz ROSOŁOWSKI*
Piotr PIERZ*

ANALYSIS OF FERRORESONANCE OSCILLATIONS IN CAPACITIVE VOLTAGE TRANSFORMER

Analysis of ferroresonance oscillations in capacitive voltage transformer is presented. For this purpose an analytical approach to ferroresonance is firstly introduced. With use of the harmonic balance method the condition for avoiding stable subharmonic oscillations of the 3rd mode is stated. In the next step the ATP-EMTP simulation based investigations are carried out to find the suppression circuit parameter (or parameters) which assure damping of the nonlinear oscillations in accordance to the requirements of the standards. Two kinds of suppression circuits designed for the considered capacitive voltage transformer construction are investigated. The possible chaotic phenomena resulting from nonlinear oscillations are also examined. The obtained results are presented and discussed.

1. INTRODUCTION

The predominant sources of voltage signals for protective, monitoring, measuring and control devices in high voltage (HV) and extra high voltage (EHV) systems are capacitive voltage transformers (CVTs) which are also named as coupling capacitor voltage transformers (CCVTs) [1]. A CVT provides a cost-effective way of obtaining a secondary voltage for HV and EHV systems [1], [2]. Its functional scheme [1]–[4] is depicted in Fig. 1. A CVT is composed of a capacitive voltage divider (C_1 and C_2 – both consisting of some capacitor elements connected in series), a compensating reactor (L_{CR}) and a step-down inductive voltage transformer (Tr) usually with two secondary windings. In the scheme of Fig. 1, besides the primary voltage (u_p) and

* Department of Electrical Power Engineering, Wrocław University of Technology, Wrocław, Poland.

secondary voltages (u_{s1}, u_{s2}) one also distinguishes the intermediate voltage (u_i), which is usually at the level of around 20 kV.

Two kinds of CVT transient conditions are taken for analysis which is aimed at evaluation of CVT transient performance:

- non-linear oscillations under saturation of a magnetic core of a CVT step-down inductive voltage transformer (Tr in Fig. 1) [1]–[9],
- discharging of a CVT internal energy during decreasing the primary voltage (u_p) which is the case of short circuits on the associated transmission line [10]–[14].

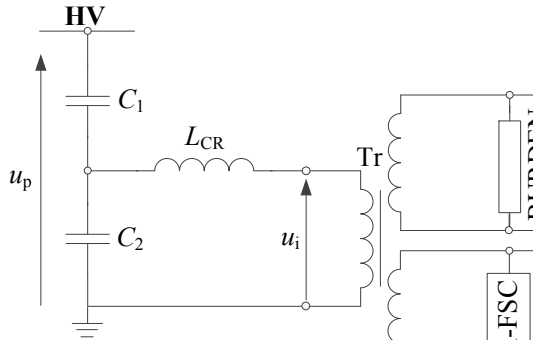

Fig. 1. Schematic diagram of CVT: C_1, C_2 – stack capacitors; L_{CR} – compensating reactor; Tr – inductive step-down transformer; A-FSC – anti-ferroresonance suppressing circuit; BURDEN – burden imposed by connected protective and other devices

Non-linear oscillations can appear when the operating point of the magnetizing characteristic of the step-down transformer is shifted to the saturation region. The energy stored in the capacitive and inductive elements of the device generate transients with low frequency of aperiodic character which could last of long period. On the other hand a sudden change of voltage at the primary terminals of the step-down transformer could cause saturation of the magnetic core what with interaction with capacitance are sources of non-linear oscillations called ferroresonance. CVTs are therefore equipped with special anti-ferroresonance circuit (A-FSC in Fig. 1) for avoiding stabilization of the sub-harmonics and also assuring adequately fast damping of the oscillations. Both, passive [3]–[7] and active [8] suppression circuits are used. Power electronic elements are utilized for constructing the active circuits [8].

In turn, the CVT generated transients under short circuits on the associated transmission line are simpler for analysis since a CVT still operates at its linear range [10]–[14]. Such transients are commonly investigated in relation to their influence of protective relays operation. This issue is out of the scope of this paper.

2. SUBHARMONIC FERRORESONANCE IN CVTS

2.1. INTRODUCTION

CVTs installed in a power system operate during normal steady state conditions within a linear range for a step-down transformer (Fig. 1). However, under some disturbances this is not so. The exploitation experiences and laboratory tests show that extensive nonlinear oscillations can be generated in the CVT circuit. Such oscillations can appear under the disturbances such as [5], [10]:

- interruption of the short-circuit in the secondary CVT winding when the protecting fuse gets blown out,
- interruption of the short-circuit at the stack capacitor C_2 due to operation of the spark gap which protects it (the spark gap is not shown in Fig. 1),
- sudden appearing of the CVT primary voltage under switching on or interruption of the short-circuit at the CVT primary side,
- increase of the CVT primary voltage due to overvoltage,
- lightning-caused ferroresonance.

2.2. DESIGN OF FERRORESONANCE SUPPRESSION CIRCUIT

The exploitation experiences and laboratory tests show that if a CVT is not equipped with a properly designed suppression circuit, the subharmonic ferroresonance phenomenon [3]–[8] can occur. Subharmonic oscillations of 3rd or 5th mode can be generated in a CVT circuit. This is also known that more severe conditions are for damping the 3rd subharmonic oscillations and thus this will be concerned further. It is desired to prevent stabilization of such subharmonics and moreover to assure their fast damping, accordingly to the requirements imposed by the international standards [9]. To achieve this goal, a special anti-ferroresonance suppression circuit has to be applied at the step-down transformer output. In Fig. 1 it is presented that such circuit is connected to the dedicated winding, i.e. separately from the burden.

As so far, there are no design methods with the calculation procedure for selecting the suppression circuit parameter (or parameters). This is so since the CVT circuit has to be considered as a non-linear circuit. This paper is aimed at providing the design method for the suppression circuit which is based on the 2-step procedure:

- preliminary selection of the circuit parameters which assure that presence of stable subharmonic oscillations of 3rd mode are not possible,
- tuning the circuit parameters which assure that the standard requirements are satisfied with the aid of digital simulation.

Knowledge of the border conditions for avoiding stable subharmonics (1st step) facilitates carrying out the 2nd step of the design.

2.3. ANALYTICAL APPROACH TO SUBHARMONIC FERRORESONANCE

Since the CVT circuit is considered as a non-linear circuit its analytical analysis limits to the steady state considerations. For this purpose the harmonic balance method [10] will be utilized. This method assumes that the steady state solution for the nonlinear circuit can be represented by a linear combination of sinusoids, then balances current and voltage sinusoids to satisfy Kirchhoff's law.

An equivalent circuit diagram of a CVT used for the harmonic balanced method in relation to the subharmonic 3rd mode is presented in Fig. 2.

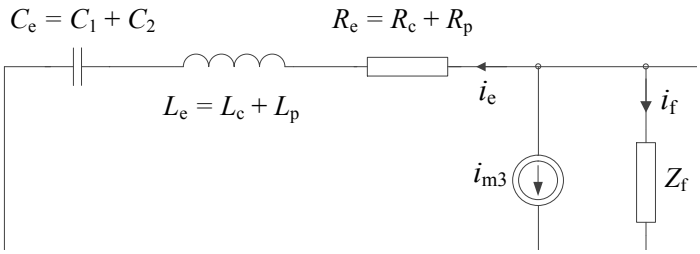

Fig. 2. Equivalent circuit diagram of CVT for studying 3rd subharmonic ferroresonance with all parameters related to the primary side of the step-down transformer: C_e – equivalent capacitance of capacitive divider, L_e – sum of inductances of the compensating reactor and of the primary winding of the step-down transformer, R_e – analogously as L_e, i_{m3} – current source of the 3rd harmonic current, Z_f – ferroresonance suppression circuit, Z_b – burden

In analytical considerations the following polynomial approximation of a magnetizing characteristic (magnetizing current i_m as a function of linkage flux ψ) is commonly used:

$$i_m = \sum_{k=0}^{n} a_{2k+1} \psi^{2k+1} \tag{1}$$

The number of terms used in (1) is: $n + 1$ and, in general, if the higher order approximation (i.e. higher n) is used, a better accuracy is achieved. However, this results in more complex analytical analysis or even in no possibility to obtain the solution without involving numerical calculation algorithms. This is the case also for analytical considerations of subharmonic ferroresonance in CVTs dealt in this paper. Therefore, it appears that a reasonable analytical approach can be carried out with using the following 3rd order ($n = 1$) approximation of the magnetizing characteristic:

$$i_m = a_1 \psi + a_3 \psi^3 \tag{2}$$

Limiting the presence of the fundamental frequency and the subharmonic 3rd mode in the CVT circuit, the linkage flux of the step-down transformer can be expressed as:

$$\psi(t) = \Psi_1 \cos(\omega t + \varphi) + \Psi_3 \cos\left(\frac{\omega t}{3}\right) \tag{3}$$

where the unknowns are: Ψ_1, Ψ_3 – magnitudes of the linkage flux for the fundamental frequency and 3rd subharmonic, respectively; φ is the phase displacement.

Substituting (3) into (2) and expanding the products of cosine functions into their sums one obtains the magnetizing current in the following form:

$$\begin{aligned} i_{\mathrm{m}} = {} & F_1 \cos\left(\frac{\omega t}{3}\right) + F_2 \cos\left(\frac{\omega t}{3} + \varphi\right) + F_3 \cos(\omega t) \\ & + F_4 \cos(\omega t + \varphi) + F_5 \cos\left(\frac{5\omega t}{3} + \varphi\right) + F_6 \cos\left(\frac{5\omega t}{3} + 2\varphi\right) \\ & + F_7 \cos\left(\frac{7\omega t}{3} + 2\varphi\right) + F_8 \cos(3\omega t + 3\varphi) \end{aligned} \tag{4}$$

where:

$$F_1 = a_1\Psi_3 + \frac{3}{2}a_3\Psi_1{}^2\Psi_3 + \frac{3}{4}a_3\Psi_3{}^2, \quad F_2 = \frac{3}{4}a_3\Psi_1\Psi_3{}^2,$$

$$F_3 = \frac{1}{4}a_3\Psi_1\Psi_3{}^2, \quad F_4 = a_1\Psi_1 + \frac{3}{4}a_3\Psi_1{}^3 + \frac{3}{2}a_3\Psi_1\Psi_3{}^2,$$

$$F_5 = \frac{3}{4}a_3\Psi_1\Psi_3{}^2, \quad F_6 = \frac{3}{4}a_3\Psi_1{}^2\Psi_3,$$

$$F_7 = \frac{3}{4}a_3\Psi_1{}^2\Psi_3, \quad F_8 = \frac{1}{4}a_3\Psi_1{}^3.$$

The 3rd subharmonic of the magnetizing current (4) taken for further analysis is thus equal:

$$i_{\mathrm{m3}}(t) = F_1 \cos\left(\frac{\omega t}{3}\right) + F_2 \cos\left(\frac{\omega t}{3} + \varphi\right) \tag{5}$$

Since the 3rd subharmonic of the linkage flux (3) is being assumed as:

$$\psi_3(t) = \Psi_3 \cos\left(\frac{\omega t}{3}\right) \tag{6}$$

the 3rd subharmonic of the voltage drop across the magnetizing branch equals:

$$u_3(t) = \frac{\mathrm{d}\psi_3(t)}{\mathrm{d}t} = -\frac{\omega}{3}\Psi_3 \sin\left(\frac{\omega t}{3}\right) \tag{7}$$

Applying the complex number analysis for the 3rd subharmonic to the CVT equivalent circuit (Fig. 2) one obtains:

$$\underline{I}_{\mathrm{m3}} = -\underline{Y}_3 \underline{U}_3 \tag{8}$$

The admittance $\underline{Y}_3$ for the 3rd subharmonic from (8) is determined by the parameters of three branches which are in parallel to the magnetizing branch (Fig. 2):

$$\underline{Y}_3 = \frac{1}{\dfrac{3}{\mathrm{j}\omega C_\mathrm{e}} + \mathrm{j}\dfrac{\omega}{3} L_\mathrm{e} + R_\mathrm{e}} + \frac{1}{Z_\mathrm{f}\left(\mathrm{j}\dfrac{\omega}{3}\right)} + \frac{1}{Z_\mathrm{b}\left(\mathrm{j}\dfrac{\omega}{3}\right)} \tag{9}$$

Rewriting (8) with use of (5) and (7) yields the following complex number equation:

$$\Psi_3\left(a_1 + \frac{3}{2}a_3\Psi_1^{\,2} + \frac{3}{4}a_3\Psi_3^{\,2} + \frac{3}{4}a_3\Psi_1\Psi_3 \mathrm{e}^{\mathrm{j}\varphi}\right) = -\mathrm{j}\underline{Y}_3 \frac{\omega}{3}\Psi_3 \tag{10}$$

Resolving (10) into the real and imaginary parts one obtains the following set of two equations:

$$\begin{aligned} \frac{3}{4}a_3\Psi_1\Psi_3\cos(\varphi) &= -\frac{\omega}{3}\,\mathrm{real}(\mathrm{j}\underline{Y}_3) - a_1 - \frac{3}{2}a_3\Psi_1^{\,2} - \frac{3}{4}a_3\Psi_3^{\,2} \\ \frac{3}{4}a_3\Psi_1\Psi_3\sin(\varphi) &= -\frac{\omega}{3}\,\mathrm{imag}(\mathrm{j}\underline{Y}_3) \end{aligned} \tag{11}$$

After determining $\cos(\varphi)$ and $\sin(\varphi)$ from (11) and utilizing Pythagorean trigonometric identity, after performing tedious derivations, one obtains the following equation for the sought magnitude of the 3rd subharmonic of the linkage flux:

$$\left(\frac{9}{16}a_3^{\,2}\right)\Psi_3^{\,4} + \left(\frac{3}{2}Ma_3 - \frac{9}{16}a_3^{\,2}\Psi_1^{\,2}\right)\Psi_3^{\,2} + \left(M^2 + N^2\right) = 0 \tag{12}$$

where for the purpose of the formula shortening the following quantities have been introduced:

$$\begin{aligned} M &= \frac{\omega}{3}\,\mathrm{real}(\mathrm{j}\underline{Y}_3) - a_1 - \frac{3}{2}a_3\Psi_1^{\,2} \\ N &= \frac{\omega}{3}\,\mathrm{imag}(\mathrm{j}\underline{Y}_3) \end{aligned} \tag{13}$$

Two solutions (marked with the subscripts 1 and 2) of (12) for the magnitude of the 3rd subharmonic of the linkage flux squared (Ψ_2^3) are:

$$(\Psi_2^3)_{1,2} = \frac{1}{2}\Psi_1^2 - \frac{4}{3}\frac{M}{a_3} \pm \sqrt{\Delta_1} = 0 \tag{14}$$

where the determinant Δ_1 is expressed:

$$\Delta_1 = \frac{1}{4}\Psi_1^4 - \frac{4}{3}\frac{M}{a_3}\Psi_1^2 - \frac{16}{9}\frac{N^2}{a_3^2} \tag{15}$$

The stable 3rd subharmonic oscillations are not possible to occur if the solutions (14) are not being real numbers. This is the case if the determinant (15) is negative:

$$\Delta_1 = \frac{1}{4}\Psi_1^4 - \frac{4}{3}\frac{M}{a_3}\Psi_1^2 - \frac{16}{9}\frac{N^2}{a_3^2} < 0 \tag{16}$$

In order to determine the quantities M, N, defined in (13), which are involved in the inequality (16), it is taken into account that:

$$\begin{aligned} \text{real}(\text{j}\underline{Y}_3) &= -\text{imag}(\underline{Y}_3) \\ \text{imag}(\text{j}\underline{Y}_3) &= \text{real}(\underline{Y}_3) \end{aligned} \tag{17}$$

As a result, the quantities M, N are as follows:

$$\begin{aligned} M &= \frac{\omega}{3}\text{imag}(\underline{Y}_3) - a_1 - \frac{3}{2}a_3\Psi_1^2 \\ N &= -\frac{\omega}{3}\text{real}(\underline{Y}_3) \end{aligned} \tag{18}$$

Substitution of (18) into (16) results in the following inequality for the condition that stable 3rd subharmonic oscillations are not possible to occur:

$$\frac{7}{4}\Psi_1^4 - \frac{4}{3a_3}\left(\frac{\omega}{3}\text{imag}(\underline{Y}_3) - a_1\right)\Psi_1^2 + \frac{16}{9a_3^2}\left(\frac{\omega}{3}\text{real}(\underline{Y}_3)\right)^2 > 0 \tag{19}$$

There are the following possibilities for generating stable 3rd subharmonic oscillations, namely the parameters of the CVT linear parameters {real ($\underline{Y}_3$), imag($\underline{Y}_3$) and the coefficient a_1 used for the nonlinear characteristic approximation (2)} are such that:

- stable subharmonic oscillations are not possible to occur if the determinant (Δ_2) for the double quadratic polynomial at the left side of (19) is negative, i.e.:

$$\Delta_2 = \left(\frac{\omega}{3}\,\mathrm{imag}(\underline{Y}_3) - a_1\right)^2 - 7\left(\frac{\omega}{3}\,\mathrm{real}(\underline{Y}_3)\right)^2 < 0 \tag{20}$$

or in a compact form:

$$\mathrm{real}(\underline{Y}_3) > \frac{1}{\sqrt{7}}\left(\mathrm{imag}(\underline{Y}_3) - \frac{3a_1}{\omega}\right) \tag{21}$$

- stable subharmonic oscillations are possible to occur if the condition (21) is not satisfied, however, only if the CVT is supplied with the voltage such that the magnitude of the fundamental frequency flux linkage (Ψ_1) is from the range:

$$(\Psi_1)_1 < \Psi_1 < (\Psi_1)_2 \tag{22}$$

where: $(\Psi_1)_1$, $(\Psi_1)_2$ are two solutions of the equation obtained by comparing the left side of (16) with zero.

This is worth to mention that in case of satisfying (22) the stable 3rd order subharmonic oscillations can be generated or not. This depends on the kind of disturbance initiating the transients. This is difficult to determine analytically which disturbance will lead to generating subharmonic oscillations and which disturbance will not initiate the subharmonic ferroresonance. However, this can be checked in a simulative way.

3. QUANTITATIVE ANALYSIS OF SUBHARMONIC FERRORESONANCE IN CVT

3.1. ANALYZED CVT CONSTRUCTION

Real, existing construction of CVTs which are installed at 220 kV transmission lines in Poland is taken for quantitative analysis of subharmonic ferroresonance. Magnetizing characteristic of the step-down transformer, related to its primary side (i.e. at the intermediate voltage (u_i) level), is presented in Fig. 3. This characteristic has been approximated by the formula (1) using weighted least error square method. Assuming $n = 1$ in (1) and taking small weights for high magnetizing current we can obtain the approximation coefficients: $a_1 = 13.85\text{e}{-6}$, $a_3 = 85.9\text{e}{-10}$.

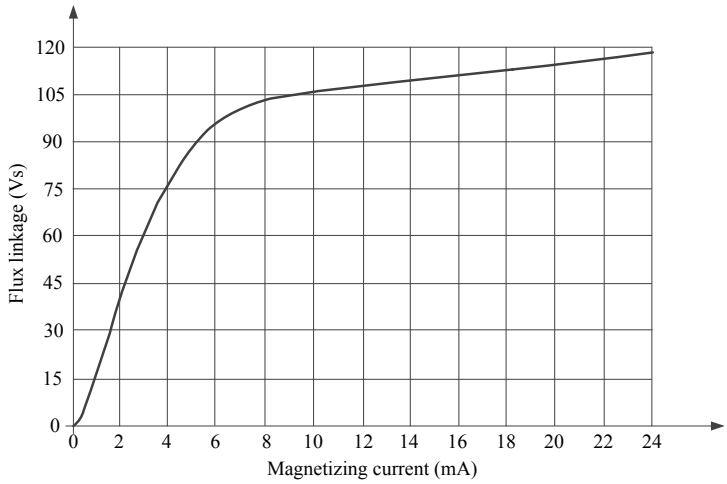

Fig. 3. Magnetizing characteristic of the step-down transformer

The other basic parameters, related to the equivalent circuit diagram from Fig. 2, are as follows: C_1 = 4.974 nF, C_2 = 47.160 nF (thus the equivalent capacitance of the capacitor divider: C_e = 52.135 nF), L_e = 194.81 H, R_e = 7242.0 Ω, L_b = 0.32 H, R_b = 133.04 Ω (including secondary side parameters of the transformer). The step-down transformer is $21000/\sqrt{3}$ V / $100/\sqrt{3}$ V / $100/\sqrt{3}$ V. The rated burden is 150 VA, however, for testing the speed of damping nonlinear oscillations according to the Polish standard [9], which is compatible with European standards, it is considered that the CVT under the test is lightly loaded with the maximal load of 5 VA. This imposes more severe conditions for damping nonlinear oscillations. According to the standard [9] the test is conducted by opening the secondary winding of the step-down transformer, which was previously short circuited. Such the test relies thus on charging of the CVT circuit with large amount of energy during the secondary winding short circuited and then by opening the winding intensive transients are occurring. This can shift the operation point on the magnetizing characteristic of the step-down transformer to its non-linear region. Damping of non-linear oscillations during such the test is considered as effective if their influence on magnitude of the CVT secondary voltage after 10 cycles (200 ms for 50 Hz fundamental frequency) from interrupting the short circuited winding is not greater than 10%. The other test details are specified in the standard [9].

Initially it is taken that the analysed CVT is equipped, as presently, with anti-ferroresonance suppression resistance (R_f) – Fig. 4a. Then it is considered that this resistance is to be replaced by the $R_fL_fC_f$ circuit with the parameters L_f, C_f tuned at the fundamental frequency resonance, thus not consuming active power during fundamental frequency steady state.

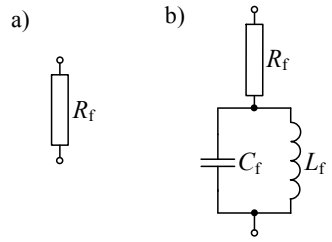

Fig. 4. Considered suppression circuits: a) suppression resistance, b) suppression circuit not consuming active power at fundamental frequency

The design of the suppression circuits is carried out with use of the 2-step procedure proposed in this paper. In the first step, the introduced analytical approach to 3rd subharmonic ferroresonance is applied for preliminary selection of the suppression circuit parameter (parameters). Then, the final selection is carried out with use of the ATP-EMTP simulation [15] for assuring that the requirements of the standard [9] are satisfied. For modelling a considered CVT construction (Fig. 1), which are manufactured as single phase units, a three-winding transformer model of the ATP-EMTP program [15] with including nonlinear magnetizing characteristic has been utilized for modelling the step-down transformer. The other elements of the CVT were modelled as *RLC* branches (Fig. 5).

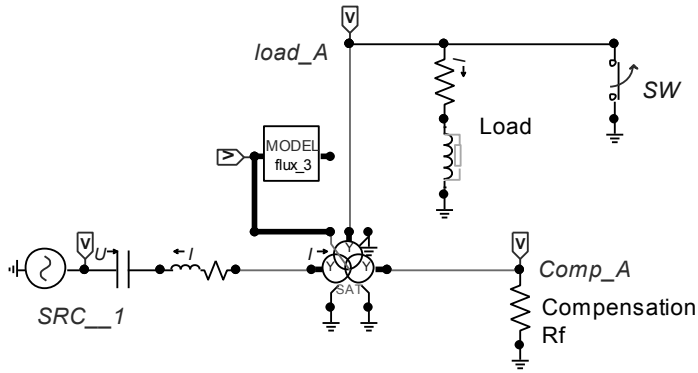

Fig. 5. ATP-EMTP model for simulation of CVT scheme

The step-down transformer is represented by the standard 3-phase 3-winding Y/y/y transformer model where only one phase (phase A) is utilized. The transformer flux linkage is calculated by integration of a magnetizing voltage in MODELS block *flux_3*. The switch SW is applied to introduce the oscillations: after being closed it is then forced to open.

Main advantage of the proposed design procedure is that having the preliminary selection from the 1st step we obtain clear indication on range of the sought parameter (parameters) of the suppression circuit which have to be set in the simulation model, instead of selecting from the whole space, applying a trial and error method. The proposed design follows in the next two subsections.

3.2. ANALYSIS OF APPLICATION OF SUPPRESSION RESISTOR R_f

Assuming that the analysed CVT is equipped with a ferroresonance suppression resistance R_f (Fig. 4a) and neglecting the CVT load (thus more severe conditions for ferroresonance suppression are taken), the admittance $\underline{Y}_3$ defined in (9) equals:

$$\underline{Y}_3 = \frac{1}{R_f} + \frac{1}{R_e + j\frac{\omega L_e}{3} + \frac{3}{j\omega C_e}} \tag{23}$$

Substituting (23) into the condition (21) one obtains that to avoid stable subharmonic oscillations of the 3rd mode one has to apply:

$$R_f < 501.45 \text{ k}\Omega \tag{24}$$

This result clearly indicates that for the considered CVT construction (with parameters as specified in the subsection 3.1) the 3rd subharmonic oscillations are possible in case if it is not equipped with anti-ferroresonance suppression resistance, i.e.: $R_f = \infty$. This is confirmed in Example 1 at Fig. 6, where the selected recorded signals of the ATP-EMTP simulation are presented. Definitely, the transients of the 3rd subharmonic nature contained in the voltage and flux signals cause that the requirements of the standard are not satisfied. This calls for equipping the CVT with adequate anti-ferroresonance circuit.

The considered CVT construction is equipped with the anti-ferroresonance resistance of the value: $R_f = 367.5$ kΩ (which corresponds to 8.33 Ω resistor connected at the $100/\sqrt{3}$ side of the step-down transformer). The resistance of the damping resistor applied is of 73% of the border value obtained in the condition (24).

ATP-EMTP simulation-based analysis for this case is presented in Example 2 at Fig. 7. The initiated transients in the recorded secondary voltage are effectively damped in such a way that their influence on voltage magnitude is no greater than 10% after 175 ms since interrupting the short circuited secondary winding. The requirements imposed by the standard [9] are definitely satisfied.

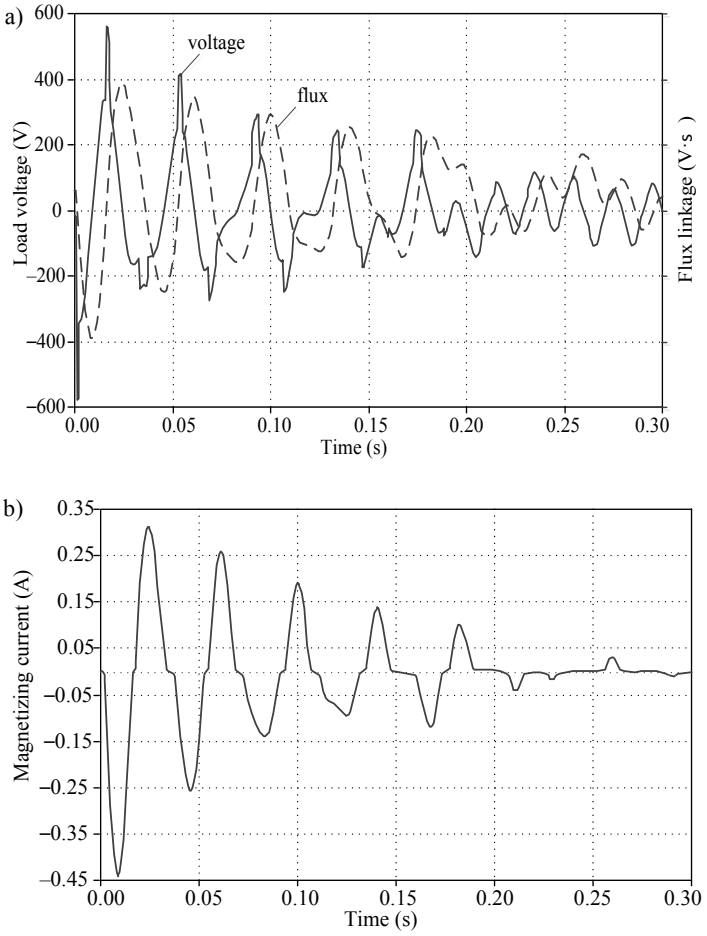

Fig. 6. Example 1 – The case of the ferroresonance test for the CVT construction with no anti-ferroresonance circuit: a) secondary voltage and flux linkage for the step-down transformer, b) its magnetizing current

The resistor R_f = 367.5 kΩ applied in the real considered CVT construction for suppressing subharmonic oscillations consumes 400 W power, which is quite big consumption in comparison to the nominal useful load (of protective and metering devices) which is designed to 150 VA. Moreover, such 400 kW permanent loading of the CVT by the anti-ferroresonance resistor is in all three phases. This is considered as a drawback of such way of damping nonlinear oscillations. From this reason it is considered further how to replace such damping resistor (Fig. 4a) with the circuit from Fig. 4b not consuming active power permanently, i.e. during steady state operation under fundamental frequency. The other option, which is not considered in this

paper, is based on applying a power electronic scheme which switches on the damping resistor only during transients, thus also not consuming active power during steady state operation under fundamental frequency.

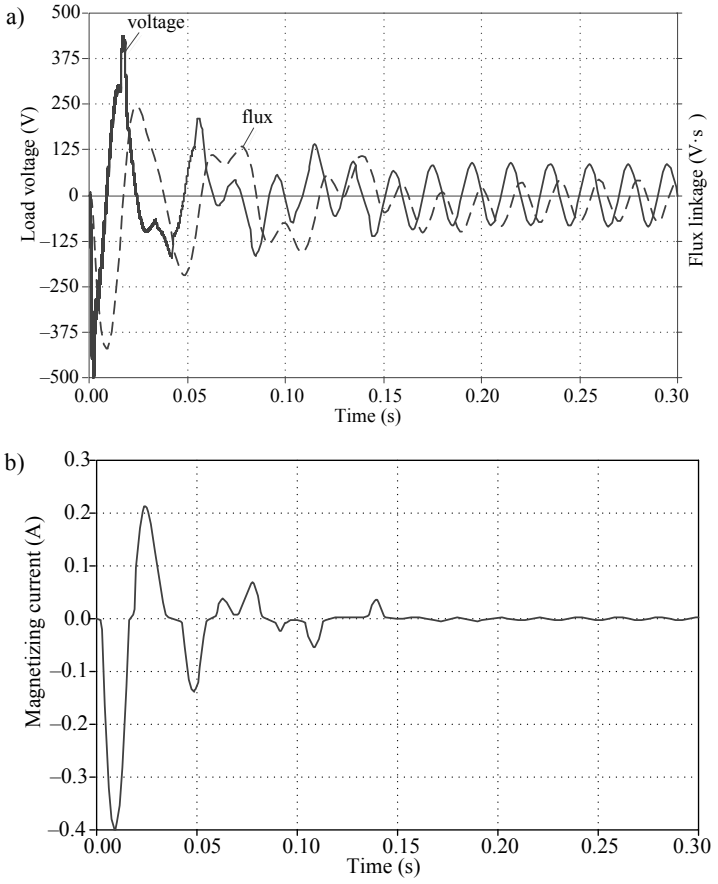

Fig. 7. Example 2 – The case of the ferroresonance test for the CVT construction with the suppression resistor R_f = 367.5 kΩ: a) secondary voltage and flux linkage for the step-down transformer, b) its magnetizing current

3.3. ANALYSIS OF APPLICATION OF SUPPRESSION CIRCUIT R_f L_f C_f

Assuming that the analysed CVT is equipped with a ferroresonance suppression circuit R_f L_f C_f (Fig. 4b) and neglecting the CVT load (thus more severe conditions for ferroresonance suppression are taken), the admittance $\underline{Y}_3$ defined in (9) equals:

$$\underline{Y}_3 = \frac{1}{R_\mathrm{f} - \mathrm{j}\frac{8}{3}\omega L_\mathrm{f}} + \frac{1}{R_\mathrm{e} + \mathrm{j}\frac{\omega L_\mathrm{e}}{3} + \frac{3}{\mathrm{j}\omega C_\mathrm{e}}} \tag{25}$$

When determining (25) it was taken into account that there is a tuning of L_f and C_f to the resonance at the fundamental frequency ($\omega^2 L_\mathrm{f} C_\mathrm{f} = 1$). For selecting the parameters of the considered suppression circuit it is assumed initially that the resistor R_f is not taking part in damping what imposes more severe conditions for the parallel connection of the elements L_f, C_f which are reactive elements and their influence is like 'increasing' the coefficient a_1 in the approximation (2), i.e. "making" the circuit more linear. Then, substituting (25) into the condition (21) one obtains that to avoid stable subharmonic oscillations of the 3rd mode the inductance L_f (recalculated for the voltage level of the primary side of the step-down transformer: $21000/\sqrt{3}$ V) has to satisfy:

$$L_\mathrm{f} < 1608.8\,\mathrm{H} \tag{26}$$

After few trials the value $L_\mathrm{f} = 1000$ H (around 60% of the border value from (26)) was taken for further analysis. Then, including the resistance R_f it has been found that there is optimal value of this resistance, i.e. the value for which the condition (21) is satisfied with the highest degree. By the term "highest degree" it is meant that the difference between the left and right sides of the inequality (21) is the highest. Thus, this feature has indicated that when carrying out the simulation based analysis for the assumed inductance ($L_\mathrm{f} = 1000$ H) one needs to search for the optimal value of R_f (Fig. 8: Example 3).

When searching for the optimal value of the resistance R_f of the circuit from Fig. 4b, the results as gathered in Table 1 have been obtained. They indicate that for the ratio $R_\mathrm{f}/(\omega L_\mathrm{f}) = 1$ the highest speed of damping is achieved. For the other values even no satisfying of the standard [9] is obtained, also including occurring stable 3rd subharmonic oscillations, what is marked by: $\propto$.

Table 1. Speed of Damping Nonlinear Oscillation Under the Ferroresonance Test of the CVT Equipped with the Suppression Circuit of Fig. 4b

L_f [H]	$\frac{R_\mathrm{f}}{\omega L_\mathrm{f}}$	Speed (ms)	Requirements satisfied?
1000	0.1	280	NO
	0.2	245	NO
	0.5	170	YES
	1.0	150	YES (optimal)
	2.0	375	NO
	5.0	$\propto$	NO
	10.0	$\propto$	NO

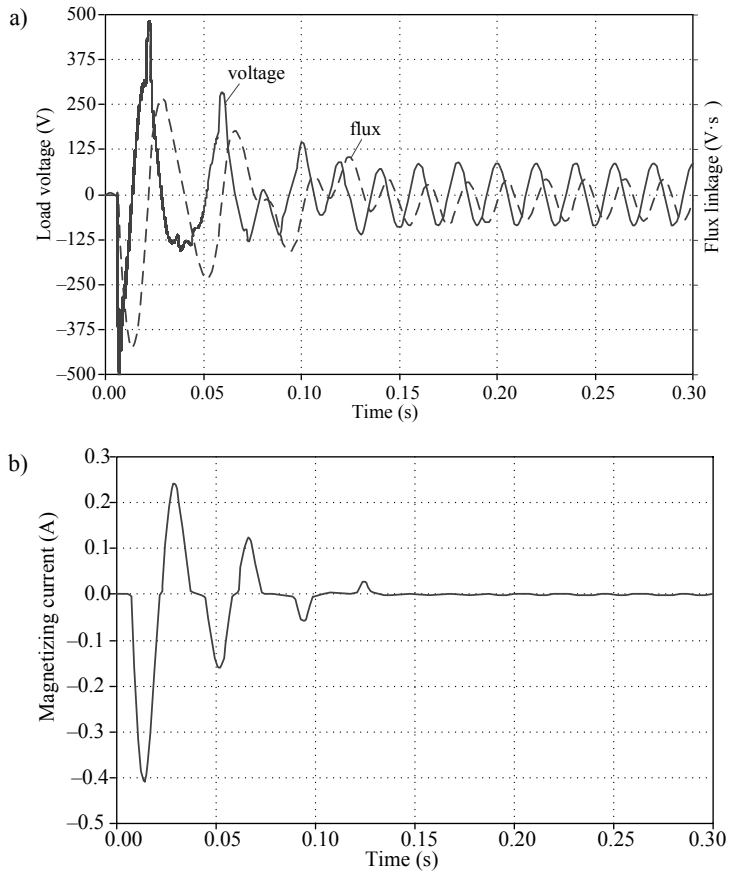

Fig. 8. Example 3 – The case of the ferroresonance test for the CVT construction with the selected suppression circuit $R_f L_f C_f$ (L_f = 1000 H, $R_f = \omega L_f$): a) secondary voltage and flux linkage for the step-down transformer, b) its magnetizing current

4. CHAOTIC OSCILLATIONS IN CVT

4.1. CLASSIFICATION OF FERRORESONANCE OSCILLATIONS

The foregoing analysis has shown that directly after the switching event in a CVT circuit, initial transient overvoltage will firstly occur and this is followed by the next phase of the transient where the process may come to at a more steady condition. Due to the non-linearity of the circuit, there can be several steady state ferroresonance responses. Depending on their spectral content, such oscillations are frequently classified as [16], [17]:

- Fundamental mode with periodic waveforms of the same period as the power system.
- Harmonic ferroresonance with periodic waveforms of a frequency multiple of the power system frequency.
- Sub-harmonic oscillations with periodic waveforms of a period sub-multiple of the power system period (with frequency of f_1/k, where: k – integer).
- Quasi-periodic ferroresonance: non-periodic waveforms with a discontinuous frequency spectrum (frequencies are defined as: $m_1 f_1 + m_2 f_2$, where m_1, m_2 – integers and f_1/f_2 is an irrational real number).
- Chaotic ferroresonance: non-periodic waveforms with a continuous frequency spectrum.

Different mathematical tools are employed to analyse the types of ferroresonance modes as: FFT or a Poincarè map [16]–[19]. The analysis given in the above sections is mainly related to sub-harmonic mode. The further part's scope is to investigate the chaotic oscillations and to identify a possible chaotic ferroresonance mode in CVT.

4.2. CHAOTIC OSCILLATIONS

Chaotic phenomenon in different physical systems is the subject of intensive study during the last several decades. Chaos (deterministic chaos) is a term used to designate the irregular behaviour of dynamical systems emerging from a strictly deterministic time evolution without any external source of fixed or probabilistic noise [20]–[22]. Such behaviour is typical for most non-linear systems. Aforementioned irregularity reveals itself in an extremely sensitive dependence on the parameters and initial conditions, which makes impossible any long-term projection of the dynamics. Mathematical tool for investigation of the chaotic phenomenon is the theory of dynamical system where an analysed system is represented by adequate set of differential equations [20].

To formulate such the equations for the CVT network let us consider the equivalent scheme as in Fig. 9, for which one can write:

$$\begin{aligned}
\frac{\mathrm{d}u_\mathrm{c}}{\mathrm{d}t} &= f_1 = \frac{1}{C} i_\mathrm{e} \\
\frac{\mathrm{d}i_\mathrm{e}}{\mathrm{d}t} &= f_2 = \frac{-1}{L_\mathrm{e}} \left(u_\mathrm{i} + u_\mathrm{c} + (R_\mathrm{e} + R_\mathrm{m}) i_\mathrm{e} + R_\mathrm{m} (i_\mathrm{b} / \vartheta + i_\mathrm{m}) \right) \\
\frac{\mathrm{d}i_\mathrm{b}}{\mathrm{d}t} &= f_3 = \frac{-1}{L_\mathrm{b}} \left((R_\mathrm{b} + R_\mathrm{m} / \vartheta^2) i_\mathrm{b} + R_\mathrm{m} (i_\mathrm{e} + i_\mathrm{m}) / \vartheta \right) \\
\frac{\mathrm{d}\psi_m}{\mathrm{d}t} &= f_4 = -R_\mathrm{m} (i_\mathrm{e} + i_\mathrm{b} / \vartheta + i_\mathrm{m})
\end{aligned} \tag{27}$$

where: $i_m = a_1\psi + a_{11}\psi^{11}$, a_1 = 4.28206e–5, a_{11} = 2.98252e–25; ϑ = 210 – transformation coefficient (the transformer is remained to compare results of calculations with simulations according to the model from Fig. 5). The switch *SW* initiates an initial condition – as in model of Fig. 5.

Equations (27) represent the non-autonomous continuous system of order $N = 4$ with external time dependent voltage source u_i. The system can be treated as autonomous one by adding explicit time dependent coordinate, obtaining $N + 1$ order system [23]. In this case the following equation was added: $\mathrm{d}\varphi/\mathrm{d}t = f_5 = \omega$, what leads to the voltage source of the form: $u_i = U\cos(\varphi(t))$ with: U = 18345.2 V, $\omega = 100\pi$ and $\varphi(0) = \pi/2$ (note that integration of this equation yields $\varphi(t) = \omega t + \pi/2$). The rest parameters of (27) are as in Subsections 3.1 and 3.2.

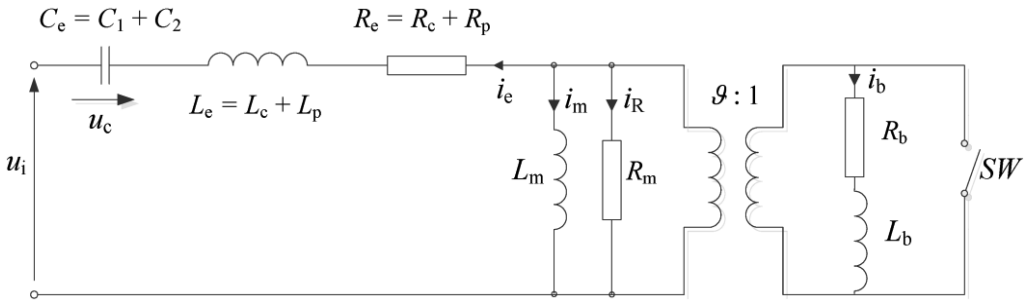

Fig. 9. Equivalent scheme of CVT

The system (27) was solved in MATLAB programme with application of the procedure `ode45` [24]. Fig. 10 gives a comparison between waveforms of the step-down flux linkage obtained from MATLAB calculation and ATP-EMTP simulation for the scheme without ferroresonance suppression circuit. One can see the significant differences in details of both the waveforms although their characters are very similar. The main source of these discrepancies is in a chaotic behaviour of the observed process. It is very sensitive to initial conditions, accuracy of a chosen integration method and other details e.g. a form of representation of the magnetizing characteristic which is different in the considered procedures: by the polynomial function $i_m = f(\psi)$ as in (27) – in the MATLAB programme, and by the piecewise-linear form – in the ATP-EMTP simulation [15].

4.3. DETECTION OF CHAOTIC PROCESS

A qualitative description of the behaviour of a non-linear circuit is usually demonstrated on phase plane. The observed trajectory gives an information on the system dynamics. This is characterised by the attraction areas to which the trajectory going

towards. It is known from the theory of dynamical systems that depending on the system features such areas can take forms of a single or various limit cycles (or even single point). Generally these cycles are called the attractors which are divided into the simple and the strange attractors [20]. Strange attractor is also called the chaotic attractor. Dynamics on the strange attractor is chaotic, and characterized by an extreme sensitivity to small changes in the initial conditions. For the computer simulated system it means that the calculation accuracy and the employed procedure also influences on the obtained waveforms.

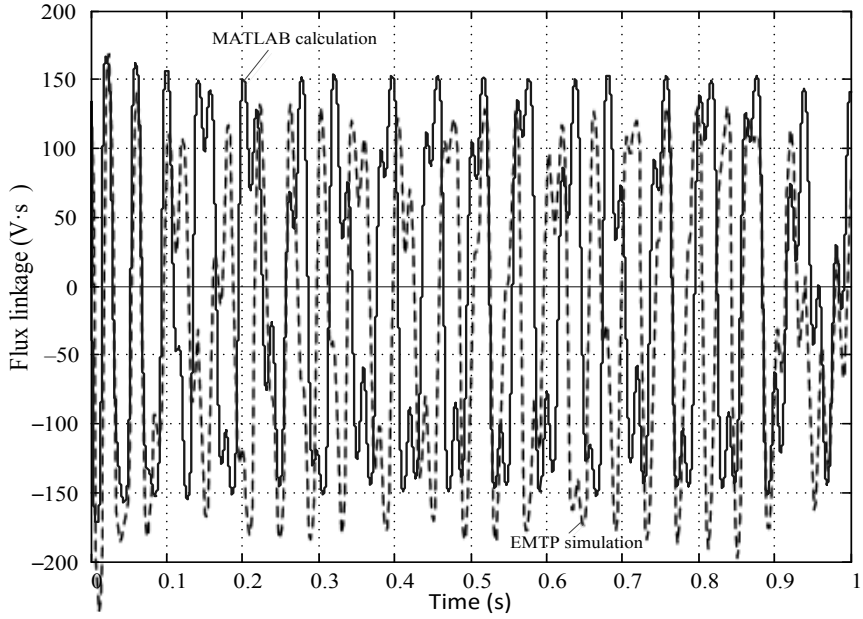

Fig. 10. Waveforms of flux linkage in step-down transformer (no suppression circuit)

As an example let us consider the phase plot in (u_c, i_e) plane for CVT scheme without the suppressing circuit (Fig. 11). After the initial transient period the trajectory evolves between two areas describing irregular cycles.

In the ferroresonant transients it is important to distinguish between the regular periodic fluctuations and the chaotic oscillations [19]. However it is easy to detect in this way a disappearance of the ferroresonance. The example is shown in Fig. 12. It is the similar phase plot as in Fig. 11 but for CVT circuit with the suppressing element in the form of resistance R_f as in Fig. 4a. One can see that after the initial transient period the trajectory describes the regular cycle for the steady state.

The chaotic evolution with a strange attractor is also characterized by so called self-similar properties, i.e., a form of a part of it is similar to the great-size (whole) set (as in fractal). Proper description of such features can be based on more general

analysis of the phase space of the system. The problem is solved by measuring the so called Lyapunov exponents or largest value from the spectrum of Lyapunov exponents [20]–[22].

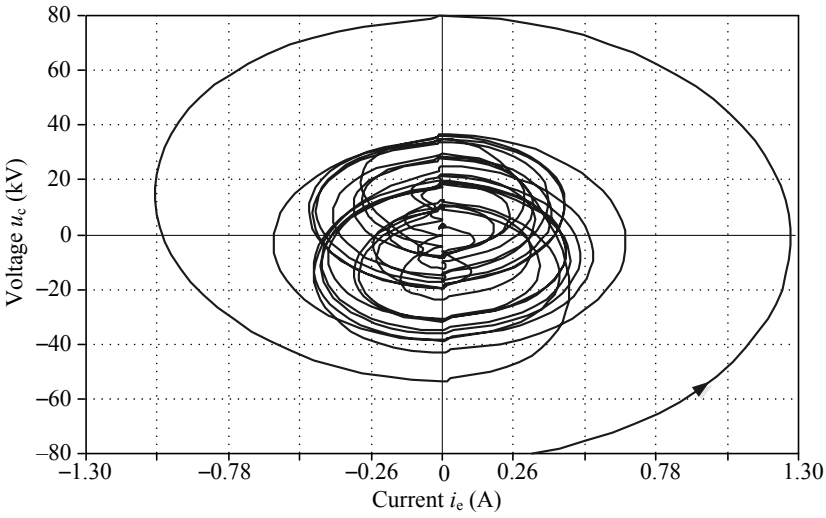

Fig. 11. Phase plot in (u_c, i_e) plane (CVT without suppressing circuit)

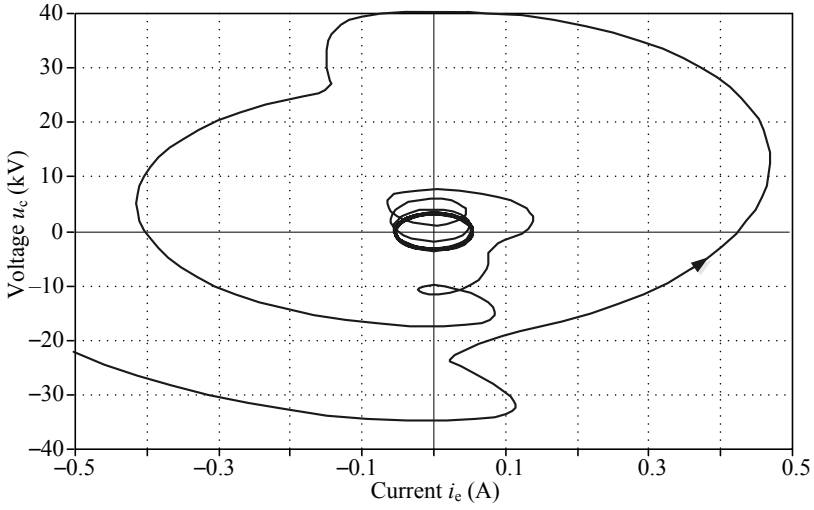

Fig. 12. Phase plot in (u_c, i_e) plane (CVT with suppressing circuit)

Lyapunov exponents quantify the exponential separation of initially close state-space trajectories and in that way characterize the amount of chaos in a system.

In a chaotic state the nearby trajectories (or initially close points) diverge exponentially, which can be quantitatively estimated by the Lyapunov exponent. The idea can be easily explained for one-dimensional discrete mapping at some interval [22]:

$$x_{n+1} = f(x_n) \tag{28}$$

Consider the evolution of (28) starting with slightly different initial conditions: x_0 and $x_0 + \Delta x_0$. The distance after n iterations can be defined as:

$$\Delta x_n = \left| f^n(x_0 + \Delta x_0) - f^n(x_0) \right| \tag{29}$$

For large n this can be estimated as [22]:

$$\Delta x_n \approx \Delta x_0 \mathrm{e}^{\lambda} \tag{30}$$

where λ is the Lyapunov exponent.

A positive Lyapunov exponent defines a chaotic trajectory. Normally, such a trajectory overlays a certain phase plane region and the Lyapunov exponent describes this region, regardless of the initial condition. Each coordinate in an N-order autonomous system described by a set of state equations can be characterized by separate Lyapunov exponent. Negative values of the Lyapunov exponent indicate stability, and positive values chaotic evolution, where λ measures the speed of exponential divergence of adjacent trajectories. The system is chaotic even if one Lyapunov exponent approaching positive value.

The methods for calculation of the Lyapunov exponents were the subject of the intensive research some years ago. Practical procedures can be found in the literature. They are adjusted to estimation of the Lyapunov exponent from the system equations [21], [22], [26] or from the recorded waveforms [21], [22], [25]. Employing the first mentioned procedure the user has to prepare a state model equations and adequate Jacobian of the transition matrix. Considering the CVT scheme with the equations (27) we can obtain:

$$\frac{\mathrm{d}}{\mathrm{d}t}\mathbf{x} = \mathbf{F}(\mathbf{x}), \qquad \mathbf{J}(\mathbf{F}) = \frac{\partial}{\partial \mathbf{x}}\mathbf{F} \tag{31}$$

where:

$$\mathbf{x} = \begin{bmatrix} u_c & i_e & i_b & \psi & \varphi \end{bmatrix}^T,$$

$$\mathbf{F}(\mathbf{x}) = \begin{bmatrix} f_1(\mathbf{x}) & f_2(\mathbf{x}) & f_3(\mathbf{x}) & f_4(\mathbf{x}) & f_5(\mathbf{x}) \end{bmatrix}^T,$$

$$\mathbf{J}(\mathbf{F}) = \begin{bmatrix} 0 & \frac{1}{C} & 0 & 0 & 0 \\ \frac{-1}{L_e} & \frac{-(R_e+R_m)}{L_e} & \frac{-R_m}{L_e\vartheta} & \frac{-R_m p_m}{L_e} & \frac{U\sin(\varphi)}{L_e} \\ 0 & \frac{-R_m}{L_b\vartheta} & \frac{-(R_b+R_m/\vartheta^2)}{L_b} & \frac{-R_m p_m}{L_b\vartheta} & 0 \\ 0 & -R_m & -R_m/\vartheta & -R_m p_m & 0 \\ 0 & 0 & 0 & 0 & 0 \end{bmatrix},$$

$$p_m = \frac{\mathrm{d}i_m}{\mathrm{d}\psi} = a_1 + 11a_{11}\psi^{10}.$$

All the network parameters are as in Subsections 3.1 and 3.2.

Details on the employed procedure in MATLAB can be found in [26]. The MATLAB programme adopted to the considered here CVT scheme is placed in [27].

Dynamics of the Lyapunov exponents for the CVT scheme without supressing circuit is presented in Fig. 13. After a short irregular transition the largest exponent λ_1 tends to value of 23.17 at the end of the showed section. The exponent λ_5 characterizes the regular component of angle φ and therefore is keeping of zero value. The exponent λ_4 takes a great negative value and is not presented in the figure.

Results of the Lyapunov exponents calculation for the same scheme but with the supressing circuit are presented in Fig. 14. This time, after a short transition the largest exponents λ_1 and λ_2 lead to some close negative values. This is typical for the stable network.

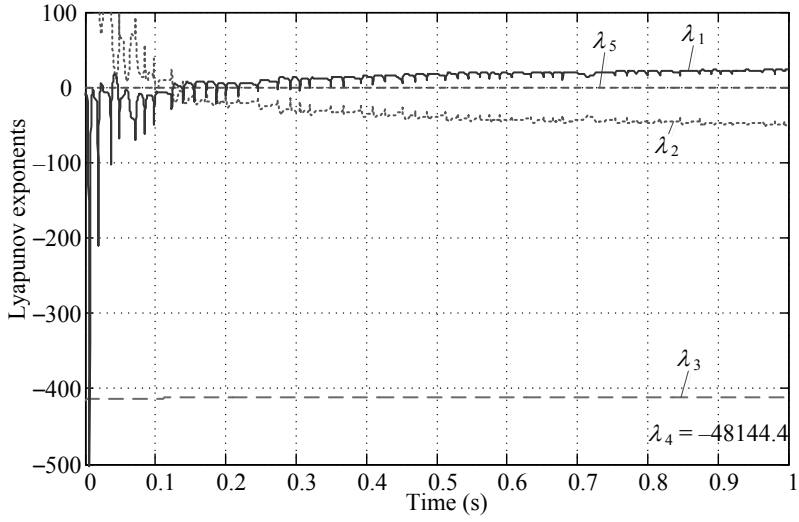

Fig. 13. Dynamics of Lyapunov exponents (CVT without suppressing circuit)

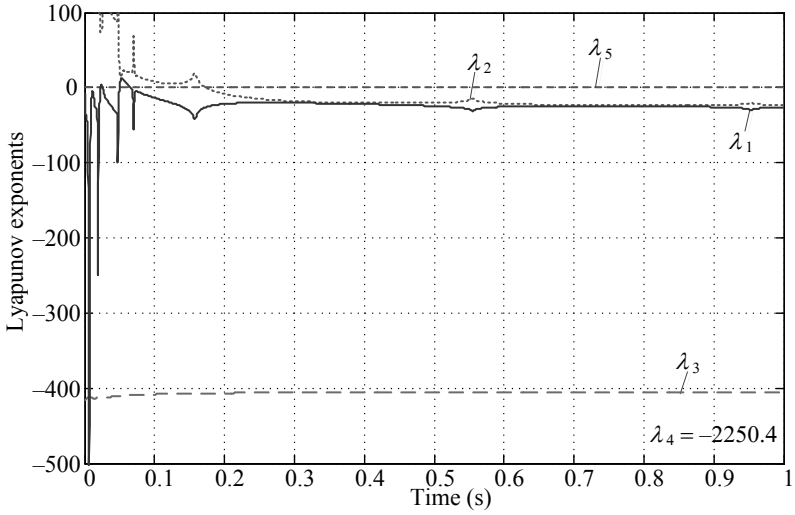

Fig. 14. Dynamics of Lyapunov exponents (CVT with suppressing circuit)

In the last calculation, the supressing circuit was included into the scheme in the form of the resistance R_f placed as parallel to the resistance R_m (Fig. 9). It is equivalent to simple reducing the value of R_m without any changing in the scheme and its set of equations.

5. CONCLUSIONS

Analysis of ferroresonance oscillations in CVT scheme has been presented. The main objective of the provided investigation was to formulate conditions for suppression of such oscillations. The 2-step procedure for designing the anti-ferroresonance suppression circuits for capacitive voltage transformers has been proposed.

The first step of the design is based on analytical approach to subharmonic ferroresonance of 3rd mode. The harmonic balance method and the 3rd order polynomial approximation of the nonlinear magnetizing characteristic have been applied. As a result, the condition stating when stable subharmonic oscillations of 3rd mode are not possible to occur has been derived.

The second step of the design is based on ATP-EMTP simulation of the ferroresonance test according to the national standard. Taking the condition derived in the first step, the final selection of the suppression circuit parameter (or parameters) is facilitated. Instead of selecting from the whole space for the parameters, the selection is to be carried out within the range where the parameters guarantee that stable subhar-

monic oscillations are not possible to occur. As a result of some limited trials the ferroresonance suppression circuit is designed to have desired speed of damping for nonlinear oscillations, i.e. as required by the standard.

Real, existing construction of CVTs has been taken for quantitative analysis. Two types of ferroresonance suppression circuits have been designed. It was shown that the presented analytical approach to subharmonic ferroresonance considerably facilitates the design of the ferroresonance suppression circuits.

Analysed ferroresonance oscillations can be divided into a few different modes depending on some specific time and spectral characteristics. It was shown that in the CVT scheme without supressing circuit one can also observe chaotic oscillations. Generally, chaotic ferroresonant behaviour depends on various parameters of the system: voltage source amplitude, capacitance and resistance, transformer core magnetic characteristic representation or initial conditions. Detection of chaotic phenomena can be provided by estimation of the Lyapunov exponents. It was shown that such oscillations can really exist in the CVT circuit.

ACKNOWLEDGMENTS

This paper was realized within NCBR project: ERA-NET, No. 1/SMARTGRIDS/2014, acronym SALVAGE, "Cyber-Physical Security for the Low-Voltage Grids".

REFERENCES

[1] ZADEH H.K., LI Z., *A compensation scheme for CVT transient effects using artificial neural network*, Electric Power Systems Research, 2008, 78, 30–38.

[2] SAHA M.M., IZYKOWSKI J., ROSOLOWSKI E., *Fault Location on Power Networks*, Springer, London 2010.

[3] ZANG W., SHU G., FENG Z., UNBEHAUEN R., *Digital simulation models of a capacitor voltage transformer*, Electrical Engineering, 2005, 87, 237–244.

[4] FERNANDES D. JR., NEVES W.L.A., VASCONCELOS J.C.A., *Coupling capacitor voltage transformer: A model for electromagnetic transient studies*, Electric Power Systems Research, 2007, 77, 125–134.

[5] BAKAR A.H.A., RAHIM N.A., ZAMBRI M.K.M., *Analysis of lightning-caused ferroresonance in Capacitor Voltage Transformer (CVT)*, Electrical Power and Energy Systems, 2011, 33, 1536–1541.

[6] MIGUEL A., OLGUÍN-BECERRIL, ANGELES-CAMACHO C., FUERTE-ESQUIVEL C.R., *Ferroresonance in subharmonic 3rd mode in an inductive voltage transformer, a real case analysis*, Electrical Power and Energy Systems, 2014, 61, 318–325.

[7] ABBASI A., SEIFI A., *Fast and perfect damping circuit for ferroresonance phenomena in coupling capacitor voltage transformers*, Elect. Power Compon. Syst., March 2009, Vol. 37, No. 4, pp. 393–402.

[8] CHAKRAPANIA V., SWARUP K.S., *Estimation of electronic suppression circuit resistance for protective relaying applications*, Electric Power Components and Systems, 43(3): 282–297, 2015.

[9] Polish Standard: PN-EN 61869-5:2011 – *Instrument transformers, Part 5: Detailed requirements for capacitor voltage transformers* (English version).

[10] IŻYKOWSKI J., WISZNIEWSKI A., *Damping of nonlinear oscillations in capacitive voltage transformers*, Przegląd Elektrotechniczny (Electrical Review), 1974, nr 1, pp. 20–23 (in Polish).
[11] IZYKOWSKI J., KASZTENNY B., ROSOLOWSKI E., SAHA M.M., HILLSTROM B., *Dynamic compensation of capacitive voltage transformers*, IEEE Trans. Power. Delivery, January 1998, Vol. 13, No. 1, pp. 116–122.
[12] KASZTENNY B., SHARPLES D., ASARO V., POZZUOLI M., *Distance relays and capacitive voltage transformers balancing speed and transient overreach*, Proceedings 53rd Annual Conference for Protective Relay Engineering, Ontario, Canada.
[13] COSTELLO D., ZIMMERMAN K., *CVT transients revisited distance, directional overcurrent and communications-assisted tripping concerns*, 65th Annual Conference for Protective Relay Engineers, College Station, TX, 2–5 April 2012, pp. 73–84.
[14] AJAEI F.B., SANAYE-PASAND M., DAVARPANAH M., REZAEI-ZARE A., IRAVANI R., *Mitigating the impacts of CCVT subsidence transients on the distance relay*, IEEE Trans. Power Del., April 2012, Vol. 27, No. 2, pp. 497–505.
[15] DOMMEL H., *ElectroMagnetic Transients Program*, BPA, Portland, Oregon, 1986.
[16] FERRACI P., *Ferroresonance*, Cahier technique no. 190, Groupe Schneider, March 1998.
[17] VAL ESCUDERO M., DUDURYCH I., REDFERN M.A., *Characterization of ferroresonant modes in HV substation with CB grounding capacitors*, Electric Power Systems Research, 2007, 77, 1506–1513.
[18] SOWA P., ŁUSZCZ K., *Chaotic behavior in a power system following ferroresonance*, Proceedings of the 14th International Scientific Conference Electric Power Engineering, 2013, pp. 79–82.
[19] FORDOEI H.R.A., GHOLAMI A., FATHI S.H., ABBASI A., *Chaotic oscillations control in the voltage transformer including nonlinear core loss model by a nonlinear robust adaptive controller*, Electrical Power and Energy Systems, 2013, 47, 280–294.
[20] SKIADAS C.H., SKIADAS C., *Chaotic Modelling and Simulation. Analysis of Chaotic Models, Attractors and Form*, CRC Press, Taylor & Francis Group, 2009.
[21] PARKER T.S., CHUA L.O., *Practical numerical algorithms for chaotic systems*, Springer-Verlag, 1989. Available in: http://link.springer.com/book/10.1007/978-1-4612-3486-9.
[22] KORSCH H.J., JODL H.-J., HARTMANN T., *Chaos. A Program Collection for the PC*, Springer-Verlag, Berlin, Heidelberg 2008.
[23] ALLIGOOD K.T., SAUER T.D., YORKE J.A., *Chaos – an introduction to dynamical systems*, Springer-Verlag, New York, Inc., 1996.
[24] *MATLAB user's guide*, The Math Works, Inc., 2000.
[25] ROSENSTEIN M.T., COLLINS J.J., DE LUCA C.J., *A practical method for calculating largest Lyapunov exponents from small data sets*, Physica D., 1993, 65, 117–134.
[26] KUZNETSOV N., MOKAEV T.N., VASILYEV P.A., *Numerical justification of Leonov conjecture on Lyapunov dimension of Rossler attractor*, Comm. in Nonl. Sci and Num. Simul., 2014, 19(4), pp. 1027–1034. The programme is also available in: http://www.math.spbu.ru/user/nk/PDF/Lyapunov-exponent-Sign-inversion-Perron-effects-Chaos.pdf
[27] *MATLAB programme for Lyapunov exponents calculation adopted to the CVT circuit*. Available in: http://zas.pwr.edu.pl/files